Journal of Neonatal Surgery
ISSN(Online): 2226-0439
Vol. 14, Issue 19s (2025)
https://www.jneonatalsurg.com

OPEN ACCESS

A Novel Approach for Diabetic Retinopathy Detection Using Sine Cosine Algorithm-Optimized Neural Network Classifier

Uttam Babu Jadhav[1], Dr. Nirupma Tiwari[2], Dr. Rajesh Kumar Nagar[3]

[1]Ph.D. Scholar, SAGE University, Indore, India

[2]Associate Professor, Computer Science & Engineering, SAGE University, Indore, India

[3]Associate Professor, Institute of Engineering & Technology, SAGE University, Indore, India

Email ID: uttamjadhav29@gmail.com, Email ID: nirupma.tiwari1974@gmail.com, Email ID: errajesh973@gmail.com

Cite this paper as: Uttam Babu Jadhav, Dr. Nirupma Tiwari, Dr. Rajesh Kumar Nagar, (2025) A Novel Approach for Diabetic Retinopathy Detection Using Sine Cosine Algorithm-Optimized Neural Network Classifier. *Journal of Neonatal Surgery*, 14 (19s), 350-363.

ABSTRACT

This research introduces a comprehensive methodology for diabetic retinopathy (DR) detection and classification by integrating advanced image processing techniques with machine learning models. The proposed approach consists of several key stages: image acquisition, contrast enhancement, blood vessel extraction, optic disc extraction, lesion candidate extraction, feature extraction, and classification using an optimized neural network. Initially, retinal images are acquired and enhanced using contrast techniques such as Histogram Equalization to improve visibility. Blood vessel extraction is performed using Gabor filtering, which efficiently highlights vessel structures through multi-scale and multi-orientation filters. After vessel extraction, optic disc extraction is carried out to isolate this key anatomical feature, followed by lesion candidate extraction to detect potential DR-related lesions. Feature extraction is then performed using Histogram of Oriented Gradients (HOG) and Local Binary Patterns (LBP), capturing gradient and texture information, respectively. Finally, a neural network classifier, optimized using the Sine Cosine Algorithm (SCA), is employed to classify the severity of DR. The methodology is validated using the DRIVE and FIRE datasets, achieving a maximum classification accuracy of 96.83%, demonstrating the superior performance of the SCA-NN approach over traditional neural network models.

Keywords: *Diabetic Retinopathy, HOG, LBP, Neural Network, Sine Cosine Algorithm.*

1. INTRODUCTION

Diabetic retinopathy (DR) is a severe complication of diabetes mellitus, marked by damage to the retinal blood vessels that can lead to vision impairment or blindness if left untreated. As diabetes prevalence rises globally, DR has become a significant public health concern, driving the need for effective and scalable screening and diagnostic strategies. Traditional DR diagnosis methods rely on manual inspection of retinal images by ophthalmologists, a process prone to variability and time constraints. Automated systems leveraging image processing and machine learning offer promising solutions to overcome these challenges, providing both accuracy and scalability for DR detection.

Recent advances in image processing and machine learning techniques have paved the way for the automated analysis of retinal images. In particular, contrast enhancement, blood vessel extraction, optic disc identification, lesion detection, and advanced classification algorithms have demonstrated potential in improving the precision of DR diagnosis. Contrast enhancement plays a vital role in making subtle pathological features more visible, thereby improving the overall diagnostic process. Blood vessel extraction, crucial for detecting vascular abnormalities, and optic disc extraction, necessary for distinguishing anatomical structures from pathological features, are key steps in the automated analysis. Lesion candidate extraction further aids in the identification of abnormal retinal regions that signal DR progression. Additionally, sophisticated classification algorithms, optimized using metaheuristic techniques, can significantly improve the accuracy of DR severity classification.

This research paper proposes a comprehensive methodology for DR detection, integrating contrast enhancement, blood vessel extraction, optic disc extraction, lesion detection, feature extraction, and an optimized neural network classifier. The main components of the proposed approach are as follows:

- Contrast Enhancement: To enhance retinal image quality, techniques such as Histogram Equalization and adaptive contrast stretching are applied. These methods improve the visibility of important features like

microaneurysms and hemorrhages, ensuring that critical structures are adequately highlighted for further analysis.

- Blood Vessel Extraction: Blood vessels are extracted using Gabor filtering, which is highly effective at detecting vessel-like structures across multiple orientations and scales. This process enhances vessel features while minimizing background noise, producing precise vessel maps that are crucial for detecting DR-related vascular abnormalities.
- Optic Disc Extraction: The optic disc is isolated using specialized techniques to differentiate it from pathological features. Accurate optic disc extraction prevents false-positive identification of lesions and improves the overall reliability of the diagnostic process.
- Lesion Candidate Extraction: Potential lesion areas are identified through automated lesion candidate extraction methods, which target abnormal features such as exudates, microaneurysms, and hemorrhages—hallmarks of DR progression. This step is essential for comprehensive DR screening.
- Feature Extraction: After lesion and vessel extraction, feature extraction is performed using techniques like Histogram of Oriented Gradients (HOG) and Local Binary Patterns (LBP) to capture gradient and texture information, respectively. These features are vital for distinguishing between normal and pathological retinal regions.
- Optimized Classification Using the Sine Cosine Algorithm: A neural network classifier, optimized using the Sine Cosine Algorithm (SCA), is employed to classify retinal images into different DR severity levels. The SCA, inspired by sine and cosine functions, optimizes the neural network's weights and biases, enhancing its convergence speed and classification accuracy. The classifier is trained on a feature set derived from the HOG and LBP methods.

The primary contributions of this research include:

- Enhanced Diagnostic Accuracy: By integrating contrast enhancement, vessel and optic disc extraction, lesion detection, and optimized classification, the proposed methodology improves DR diagnosis accuracy and reliability.
- Optimized Neural Network Performance: The Sine Cosine Algorithm effectively optimizes the neural network classifier for DR detection, yielding superior classification performance.
- Comprehensive Framework: This study presents a robust framework that combines multiple advanced techniques, offering a scalable and efficient solution for automated DR screening.

The remainder of this paper is organized as follows: Section 2 reviews related work in the field of diabetic retinopathy detection and the application of image processing and machine learning techniques. Section 3 details the proposed methodology, including the image pre-processing steps, vessel extraction techniques, and the classification algorithm. Section 4 presents the experimental setup, results, and performance evaluation of the proposed approach. Finally, Section 5 concludes the paper and discusses potential future directions for research in automated DR detection.

2. LITERATURE REVIEW

The authors of [1] developed a system to detect and analyze retinal changes due to diabetic retinopathy (DR). They extracted distinctive features to differentiate between healthy and diseased images, determining DR stages. Histogram equalization was applied for brightness preservation, and segmentation was used to extract pathology variations. Using a gray level co-occurrence matrix, six features were considered, focusing on image areas and bifurcation points. Classification with a Support Vector Machine (SVM) achieved 89.2% accuracy, 85.1% sensitivity, and 85.2% specificity. In [2], global texture features were extracted and analyzed using Principal Component Analysis (PCA) and Independent Component Analysis (ICA), combined with local retinal features. These were evaluated in a multi-classifier framework, including K-Nearest Neighbors (K-NN), SVM, and artificial neural networks, reporting an accuracy of 74.6%, sensitivity of 90.1%, and specificity of 56.1%.

In [3], a Convolutional Neural Network (CNN) with a hierarchical CF-DRNet detection architecture was proposed for classifying five DR stages. It reported accuracies of 56.16% and 83.10%, sensitivities of 64.21% and 53.99%, and specificities of 87.39% and 91.22% for the IDRiD and EyePACS-Kaggle datasets, respectively. A scheme based on Contrast Limited Adaptive Histogram Equalization (CLAHE) was used in [4] for image enhancement. An EfficientNet-B5 architecture, trained and evaluated on the Messidor and IDRiD datasets, reported an AUC of 0.945 and 0.932, respectively. In [5], the Inception-V3 and InceptionResNet-V2 architectures were used for five-class binary classification, achieving AUC values of 0.958 for Messidor-1 and 0.92 for Messidor-2.

In [6], a hybrid Inception-V3 and SVM architecture was applied to a private database of 200 images and the EyePACS-Kaggle dataset. Feature extraction was performed using a pre-trained CNN, and SVM was used for classification, reporting

81.5% and 90.8% sensitivity, and 71.9% and 50% specificity for the EyePACS-Kaggle and private datasets, respectively. In [7], VGG-16 and VGG-19 architectures were used on the EyePACS-Kaggle dataset, achieving 80% sensitivity, 82% specificity, and 82% accuracy. Similarly, [8] compared neural networks with backpropagation, a deep neural network, and a CNN with a VGGNet architecture, with the CNN achieving the best classification accuracy of 72.5%. In [9], CNN architectures like ResNet-50, ResNet-101, VGG-16, and Inception-V3 were evaluated on the EyePACS-Kaggle dataset, with ResNet-101 and VGG-16 performing best during training at 82% and 75% accuracy, though ResNet-101 dropped to 52% during validation.

A CNN with AlexNet architecture and a multi-instance deep learning method was tested in [10] on the EyePACS-Kaggle, Messidor, and DIARETDB1 datasets, achieving AUC values of 0.925 for Kaggle and 0.96 for Messidor. In [11], a six-layer CNN was proposed, trained on the DRIVE, DIARETDB0, and DIARETDB1 databases, reporting a classification accuracy of 96.9%, 98% sensitivity, and 93% specificity. A transfer learning approach using Inception-V3 in [12] achieved 93.49% accuracy, 96.93% sensitivity, and 95% specificity on the Messidor-2 and EyePACS-Kaggle datasets.

In [13], a five-layer CNN was designed to avoid overfitting and was compared with pre-trained networks like AlexNet, VGG-16, and SqueezeNet on the Messidor dataset. SqueezeNet achieved 94.49% accuracy, while the proposed model reached 98.15%. Overfitting, a common issue in pre-trained networks, was mitigated in the new design. In [14], a multichannel neural network using RGB image channels as inputs achieved 97.08% accuracy when using the blue channel. A fuzzy logic-based classification approach in [15] quantified microaneurysms, exudates, and blood vessels, validated on STARE, DIARETDB0, and DIARETDB1 datasets, reporting 95.63% accuracy, 95.77% sensitivity, and 94.44% specificity. In [16], SVM and K-NN classifiers were compared for DR classification, with promising results.

Despite significant advancements, key research gaps remain. Many studies focus on specific datasets or features, limiting their generalizability. While feature extraction techniques and CNNs are common, advanced preprocessing methods, like optic disc and lesion candidate extraction, and hybrid techniques (HOG and LBP), are underexplored. Additionally, the potential of hybrid models combining traditional machine learning and deep learning for DR detection across diverse datasets is not fully realized.

To address these gaps, the proposed methodology introduces an advanced DR detection and classification framework. It includes enhanced image preprocessing with contrast enhancement, vessel extraction using Gabor filtering, optic disc extraction, and lesion detection. Advanced feature extraction using HOG and LBP is integrated with a Sine Cosine Algorithm-Optimized Neural Network (SCA-NN) classifier. This approach aims to improve feature extraction and classification performance, providing a robust solution for DR detection that overcomes limitations of prior methods.

3. PROPOSED METHODOLOGY

The proposed methodology for diabetic retinopathy (DR) detection consists of several steps, each involving different image processing and classification techniques. The process starts with image acquisition and preprocessing, followed by optic disc extraction, lesion candidate extraction (lesion detection), feature extraction, and finally classification using a neural network optimized with a Sine Cosine Algorithm.

The methodology is divided into several stages: image acquisition, contrast enhancement, blood vessel extraction, optic disc extraction, lesion candidate extraction, feature extraction, and classification. Retinal images are enhanced to improve feature visibility, followed by the extraction of blood vessels using Gabor filters, optic disc extraction for proper localization, and lesion detection to identify abnormal regions in the retina. The classification is performed using a neural network optimized with the Sine Cosine Algorithm (SCA) for better performance in classifying diabetic retinopathy severity. Figure 1 outlines the flow diagram of the proposed methodology.

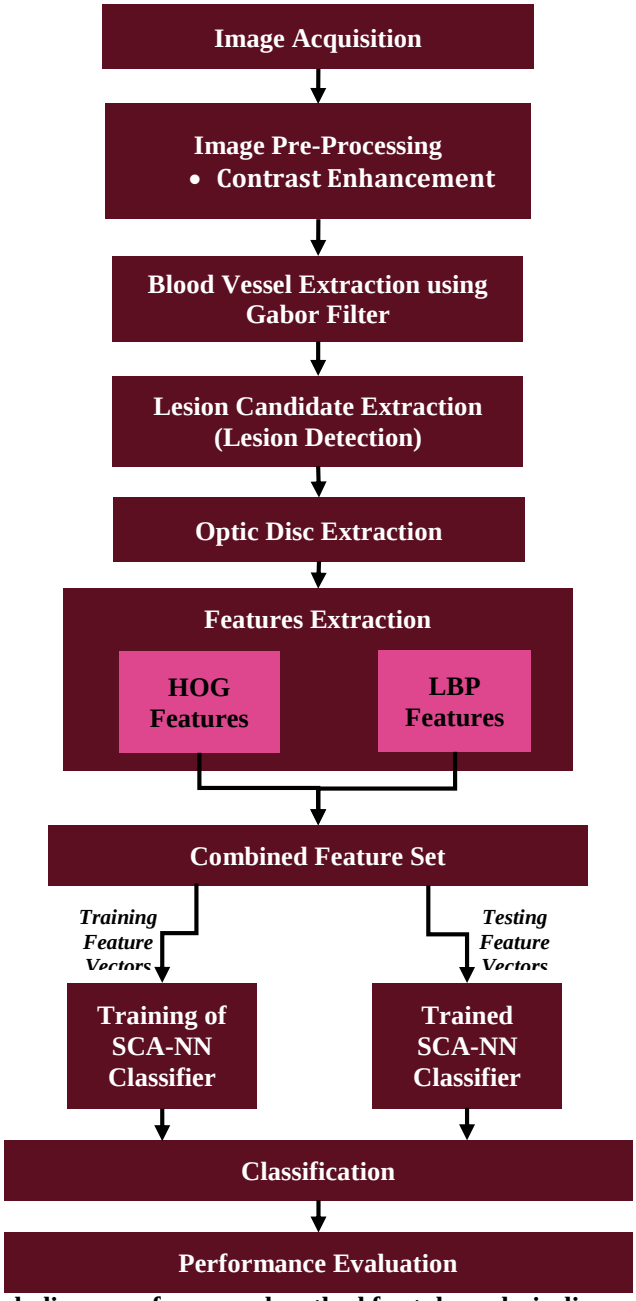

Figure 1: Block diagram of proposed method for tuberculosis diseases recognition

3.1 Image Acquisition

Image acquisition is fundamental to DR detection, involving the collection of high-resolution retinal images. These images serve as the foundation for subsequent analysis. A retinal image can be represented as a 2D matrix $I(x, y)$, where x and y denote the pixel coordinates. For color fundus images, it extends to three dimensions to include the RGB channels:

$$I(x, y) = \{I_R(x, y), I_G(x, y), I_B(x, y)\} \quad (1)$$

Here, $I_R(x, y)$, $I_G(x, y)$, and $I_B(x, y)$ represent the intensity values for the red, green, and blue channels, respectively.

This study utilizes the DRIVE database and Fundus Image Registration Dataset for training and testing, providing retinal images that facilitate the evaluation of blood vessel segmentation and lesion detection algorithms.

3.2 Image Preprocessing using Contrast Enhancement

Contrast enhancement improves the visibility of key retinal features. Histogram Equalization is applied to redistribute pixel intensities for better clarity, facilitating easier detection of blood vessels and lesions.

Histogram equalization involves the following steps:

3.2.1 Compute the Histogram

The histogram $H(r)$ of an image is a graphical representation of the frequency of each intensity value r within the image. For a given grayscale image $I(x,y)$, where $I(x,y)$ denotes the intensity value at pixel coordinates (x,y), the histogram is calculated as:

$$H(r) = \sum_{x,y} \delta(I(x,y) = r) \quad (2)$$

Where $\delta(\cdot)$ is the Dirac delta function, which is 1 if the condition inside is true and 0 otherwise.

3.2.2 Calculate the Cumulative Distribution Function (CDF)

The CDF represents the cumulative probability of pixel intensities up to a given value r. It is computed as:

$$CDF(r) = \sum_{r' \le r} \frac{H(r')}{N} \quad (3)$$

Where N is the total number of pixels in the image. The CDF provides a cumulative probability distribution of pixel intensities.

3.2.3 Map Intensity Levels

The output intensity values are determined by mapping the original intensity levels using the CDF. The enhanced image $I_{eq}(x,y)$ is obtained as:

$$I_{eq}(x,y) = round\left[(L-1) \cdot CDF\left(I(x,y)\right)\right] \quad (4)$$

Where L represents the number of intensity levels in the image (e.g., 256 for an 8-bit image). This mapping function redistributes the intensity values so that the histogram of the output image is spread across the entire range of available intensity levels.

3.3 Blood Vessel Extraction using Gabor Filtering

Blood vessel extraction is a critical step in analyzing retinal images for diabetic retinopathy (DR). Gabor filtering is an effective technique for detecting vessel-like structures due to its capability to capture edge information and texture patterns. This method leverages the Gabor filter's ability to detect specific orientations and scales, which is crucial for highlighting the tubular structure of blood vessels in retinal images.

A Gabor filter is a linear filter used to extract features related to the spatial frequency and orientation of patterns within an image. It is particularly effective in capturing vessel-like structures due to its Gaussian envelope combined with a sinusoidal wave. The Gabor filter function $g(x,y)$ is defined as:

$$g(x,y) = \exp\left(-\frac{x^2+y^2}{2\sigma^2}\right) \cdot \cos(2\pi f_0 x + \phi) \quad (5)$$

Where:

- σ is the standard deviation of the Gaussian envelope, controlling the filter's spatial extent.
- f_0 is the frequency of the sinusoidal wave, related to the scale of the detected features.
- ϕ is the phase offset, which adjusts the filter's phase.

The Gabor filter can be rotated to detect vessel structures at various orientations by modifying the x and y coordinates:

$$g_\theta(x,y) = \exp\left(-\frac{x'^2+\gamma^2 y'^2}{2\sigma^2}\right) \cdot \cos(2\pi f_0 x' + \phi) \quad (6)$$

Where:

- $x' = x\cos(\theta) + y\sin(\theta)$
- $y' = -x\sin(\theta) + y\cos(\theta)$
- θ is the orientation of the filter.
- γ is the spatial aspect ratio, which defines the ellipticity of the filter.

3.3.1 Applying the Gabor Filter

The Gabor filter is applied to the retinal image through convolution. Let $I(x,y)$ represent the original image, and $g_\theta(x,y)$ be the Gabor filter at orientation θ. The filtered image $I_{gabor}(x,y)$ is obtained by convolving $I(x,y)$ with $g_\theta(x,y)$:

$$I_{gabor}(x,y) = I(x,y) * g_\theta(x,y) \quad (7)$$

Where $*$ denotes the convolution operation. This convolution operation enhances vessel-like structures oriented at angle θ and scales corresponding to f_0.

3.3.2 Multi-scale and Multi-Orientation Filtering

To robustly detect blood vessels, multiple Gabor filters with different scales and orientations are applied to the image. The choice of scales and orientations allows the method to capture vessel structures of various sizes and directions. Let Θ represent a set of orientations and F a set of frequencies. The combined filtered image $I_{combined}(x,y)$ is computed as:

$$I_{combined}(x,y) = \max_{\theta\in\Theta, f_0\in F} I_{gabor}(x,y,\theta,f_0) \quad (8)$$

Where $I_{gabor}(x,y,\theta,f_0)$ denotes the result of applying the Gabor filter with orientation θ and frequency f_0.

3.4 Optic Disc Extraction

Step 1: Region of Interest (ROI) Detection: The optic disc (OD) is one of the brightest circular regions in retinal images. First, the image is thresholded to segment out the optic disc. The binary mask for the optic disc is represented as:

$$M_{OD}(x,y) = \begin{cases} 1 & if\ I(x,y) > T_{OD} \\ 0 & otherwise \end{cases} \quad (9)$$

Where T_{OD} is an intensity threshold that isolates the optic disc from other structures.

Step 2: Circular Hough Transform: To precisely locate the optic disc, a Circular Hough Transform (CHT) is applied. The equation of a circle is:

$$(x-a)^2 + (y-b)^2 = r^2 \quad (10)$$

Where (a,b) is the center, and r is the radius. The CHT accumulates votes for different possible circle centers and radii, and the circle with the highest votes corresponds to the optic disc.

Step 3: Masking the Optic Disc: Once the optic disc is detected, it is masked to avoid interference with lesion detection. The masked image is:

$$I_{masked}(x,y) = I(x,y)\cdot(1 - M_{OD}(x,y)) \quad (11)$$

This step removes the optic disc from further analysis by setting its intensity to zero.

3.5. Lesion Candidate Extraction (Lesion Detection)

Step 1: Candidate Region Detection: Lesions can be dark (e.g., microaneurysms) or bright (e.g., exudates) regions in the retinal image. Two separate intensity thresholding operations are applied for each type of lesion.

For dark lesions, the binary mask is:

$$M_{dark}(x,y) = \begin{cases} 1 & if\ I_{masked}(x,y) < T_{dark} \\ 0 & otherwise \end{cases} \quad (12)$$

For bright lesions, the binary mask is:

$$M_{bright}(x,y) = \begin{cases} 1 & if\ I_{masked}(x,y) > T_{bright} \\ 0 & otherwise \end{cases} \quad (13)$$

Step 2: Morphological Operations: Morphological operations such as dilation and erosion are applied to refine the lesion masks. The final mask $M_{lesions}(x,y)$ is obtained by combining the dark and bright masks:

$$M_{lesions}(x,y) = M_{dark}(x,y) + M_{bright}(x,y) \quad (14)$$

Step 3: Region Properties and Filtering: Geometric properties (e.g., size, circularity) are used to filter false positives from the detected regions. Only regions that meet certain criteria are considered true lesions.

3.6 Feature Extraction

After detecting vessels, the optic disc, and lesion candidates, the next step is feature extraction, which involves the HOG and LBP. The combination of these two feature sets captures both shape and texture information, which are essential for classification.

3.6.1 HOG Features Extraction

The Histogram of Oriented Gradients (HOG) method captures the distribution of gradient orientations in localized portions of an image, effectively representing object shapes and structures. The process involves the following steps:

Gradient Computation: First, the gradient magnitude and direction are computed for each pixel in the image. Given an image $I(x,y)$, the gradients in the x and y directions are calculated using finite differences:

$$G_x(x,y) = I(x+1,y) - I(x-1,y) \quad (15)$$

$$G_y(x,y) = I(x,y+1) - I(x,y-1) \quad (16)$$

The gradient magnitude $G(x,y)$ and direction $\theta(x,y)$ are then computed as:

$$G(x,y) = \sqrt{G_x^2(x,y) + G_y^2(x,y)} \quad (17)$$

$$\theta(x,y) = \arctan\left(\frac{G_y(x,y)}{G_x(x,y)}\right) \quad (18)$$

Orientation Binning: The image is divided into small cells (e.g., 8×8 pixels). For each cell, the gradient orientations are binned into a fixed number of orientation bins (e.g., 9 bins ranging from 0 to 180 degrees). The histogram $H_{cell}(i)$ for orientation bin i is calculated by summing the gradient magnitudes of the pixels falling into each bin:

$$H_{cell}(i) = \sum_{(x,y)\in cell} G(x,y) \cdot w_i\big(\theta(x,y)\big) \quad (19)$$

Where $w_i\big(\theta(x,y)\big)$ is a weighting function that depends on the orientation $\theta(x,y)$.

Block Normalization: To achieve invariance to changes in illumination and contrast, the histograms of the cells are grouped into larger blocks (e.g., 2×2 cells). The histograms in each block are normalized. Let H_{block} represent the concatenated histograms of the cells within a block. The normalized block histogram $H_{block,norm}$ is computed as:

$$H_{block,norm} = \frac{H_{block}}{\sqrt{\|H_{block}\|^2 + \epsilon^2}} \quad (20)$$

Where ϵ is a small constant to prevent division by zero.

Feature Vector Construction: The final HOG feature vector is constructed by concatenating the normalized histograms from all blocks across the image. This vector represents the distribution of gradient orientations in the image, capturing the shape and texture features.

3.6.2 LBP Features Extraction

LBP is a texture descriptor that captures local patterns by comparing each pixel's intensity with its neighbors.

Local Binary Pattern Calculation: For each pixel (x,y) in the image, a local neighborhood is considered (e.g., a 3×3 window). Each pixel in the neighborhood is compared to the central pixel $I(x,y)$. The LBP value is computed as:

$$LBP(x,y) = \sum_{i=0}^{P-1} s\big(I(x_i,y_i) - I(x,y)\big) \cdot 2^i \quad (21)$$

Where P is the number of pixels in the neighborhood, (x_i,y_i) are the coordinates of the neighboring pixels, and $s(\cdot)$ is a threshold function defined as:

$$s\big(I(x_i,y_i) - I(x,y)\big) = \begin{cases} 1 & if\ I(x_i,y_i) \geq I(x,y) \\ 0 & otherwise \end{cases} \quad (22)$$

Histogram of LBP Values: The image is divided into small cells (e.g., 16×16 pixels), and the LBP values are computed for each cell. A histogram $H_{cell}(l)$ of LBP values is calculated for each cell, where l represents the LBP pattern:

$$H_{cell}(l) = \sum_{(x,y)\in cell} \delta(LBP(x,y) = l) \quad (23)$$

Where $\delta(\cdot)$ is the Dirac delta function.

Block Normalization: Similar to HOG, the histograms from neighboring cells (e.g., 2×2 cells) are concatenated into blocks and normalized. The normalization process is designed to make the LBP features robust to changes in lighting and contrast:

$$H_{block,norm} = \frac{H_{block}}{\sqrt{\|H_{block}\|^2 + \epsilon^2}} \quad (24)$$

Feature Vector Construction: The final LBP feature vector is created by concatenating the normalized histograms from all blocks. This vector provides a compact representation of texture patterns in the image, highlighting local variations in pixel intensity.

3.6.3 Combined Feature Set

This phase integrates the features extracted from HOG and LBP methods to form a unified representation of the image data, enhancing the overall feature representation for classification.

Feature Vector Integration: After extracting features using HOG and LBP, their individual feature vectors are concatenated to form a combined feature vector. Let F_{HOG} and F_{LBP} represent the feature vectors derived from HOG and LBP, respectively. The combined feature vector $F_{combined}$ is constructed as:

$$F_{combined} = [F_{HOG}, F_{LBP}] \quad (25)$$

Where $[\cdot,\cdot]$ denotes concatenation. If F_{HOG} has η_{HOG} dimensions and F_{LBP} has η_{LBP} dimensions, then $F_{combined}$ will have $\eta_{combined} = \eta_{HOG} + \eta_{LBP}$ dimensions.

Feature Fusion for Classification: The combined feature vector $F_{combined}$ is then used as input to the classification algorithm. This unified feature set provides a comprehensive representation of the image, capturing both gradient and texture information, and improves the classifier's ability to distinguish between different classes or disease stages, enhancing classification accuracy and robustness.

3.7 Sine Cosine Algorithm-Optimized Neural Network Classifier

The Sine Cosine Algorithm (SCA) is a nature-inspired optimization technique used to enhance the performance of neural network classifiers. It optimizes the parameters of the neural network to achieve better classification results. This section provides a detailed description of the SCA-optimized neural network classifier, including the optimization process and its integration into neural network training.

3.7.1 Neural Network

A neural network classifier consists of multiple layers: input, hidden, and output layers. Each layer comprises neurons (nodes) that process the input data and produce predictions. The neural network can be mathematically represented as:

$$y = \sigma(W_L \cdot \sigma(W_{L-1} \cdots \sigma(W_1 \cdot x + b_1) \cdots + b_{L-1}) + b_L) \quad (26)$$

Where:

- x is the input feature vector.
- W_i and b_i are the weight matrix and bias vector for layer i.
- $\sigma(\cdot)$ is the activation function, such as ReLU or sigmoid.
- y is the output vector representing class probabilities.

3.7.2 Sine Cosine Algorithm (SCA)

The SCA is inspired by the sine and cosine functions, which mimic the natural behavior of animal movement and are used to optimize continuous functions. The SCA optimizes the neural network parameters by iteratively updating them based on the sine and cosine functions.

Initialization: Let W_t denote the weights of the neural network at iteration t. Initialize the weights randomly within a specified range:

$$W_0 = Random(Range) \quad (27)$$

SCA Update Rules: The SCA updates the weights based on sine and cosine functions to explore the solution space. The update rules are as follows:

- *Sine and Cosine Update:* The weight update for each iteration t is given by:

$$W_{t+1} = W_t + A_t \cdot \sin(B_t \cdot C_t) \cdot (W_{best} - W_t) \quad (28)$$

Where:

  - A_t is the amplitude of the sine function, which decreases over time to ensure convergence:

$$A_t = A_0 \cdot \left(1 - \frac{t}{T}\right) \quad (29)$$

  - B_t is the frequency of the sine function, which adjusts the exploration rate:

$$B_t = B_0 \cdot \left(1 - \frac{t}{T}\right) \quad (30)$$

  - C_t is a random vector with values between 0 and 1, which introduces randomness in the update process.
  - W_{best} represents the best solution found so far.

- *Position Update:* Additionally, the position update rule is given by:

$$W_{t+1} = W_t + A_t \cdot \cos(B_t \cdot C_t) \cdot (W_{best} - W_t) \quad (31)$$

Termination Criteria: The SCA iteration continues until a stopping criterion is met, such as a maximum number of iterations T or convergence to a satisfactory solution.

3.7.3 Integration with Neural Network Training

The optimized weights obtained from the SCA are used to train the neural network. The training process involves minimizing

a loss function, such as cross-entropy loss, which measures the difference between predicted probabilities and actual class labels:

$$L(y, \hat{y}) = -\sum_{i=1}^{C} y_i \cdot \log(\hat{y}_i) \quad (32)$$

Where y is the true label vector, $\hat{y}$ is the predicted probability vector, and C is the number of classes.

Backpropagation: The gradient of the loss function with respect to the network parameters is computed using backpropagation:

$$\nabla_W L = \frac{\partial L}{\partial W} \quad (33)$$

The gradients are used to adjust the weights of the neural network, which are optimized further by the SCA.

Optimization: The neural network is trained using the optimized weights, and performance is evaluated using metrics such as accuracy, precision, recall, and F1-score.

The integration of SCA with neural network training enhances the classifier's performance by providing an optimized set of weights that improves the network's ability to classify diabetic retinopathy stages accurately.

4. SIMULATION AND RESULTS

4.1 Dataset

Image databases are essential for the development of retinal image processing algorithms, providing a means for researchers to evaluate and compare new methods against established benchmarks. This section outlines the various databases utilized in our study.

DRIVE Image Database: The DRIVE image database comprises 40 color fundus images, with 7 displaying pathological features. These images were captured using a non-mydriatic Canon RC5 retinograph, offering a 45-degree field of view (FOV). Each image is stored in JPEG format with dimensions of 768×584 pixels. The dataset is split into two parts: 20 images are used for training purposes, and the remaining 20 are used for testing. Two experienced ophthalmologists performed manual segmentation of the vascular network.

Fundus Image Registration Dataset (FIRE): The FIRE dataset consists of 129 retinal images forming 134 pairs of images. These pairs are categorized into three groups based on their characteristics. The images were captured using the Nidek AFC-210 fundus camera, which provides a 45-degree FOV and captures images at a resolution of 2912×2912 pixels. The dataset includes images from 39 patients, collected at the Papageorgiou Hospital at Aristotle University of Thessaloniki, Greece.

4.2 Results

The following figures illustrate the various stages of the lesion extraction and false lesion candidate removal process in diabetic retinopathy detection:

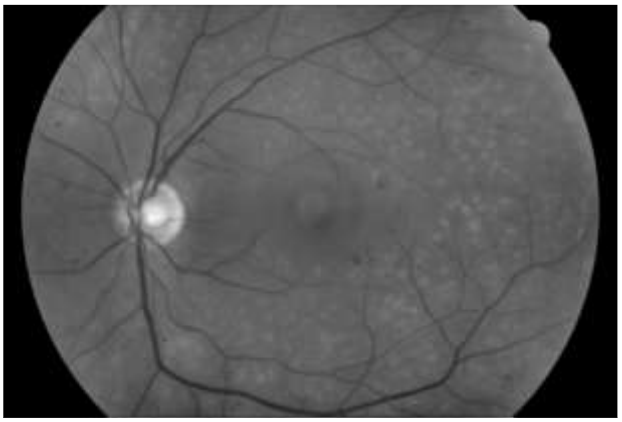

Figure 2: Lesion extraction – input green color band

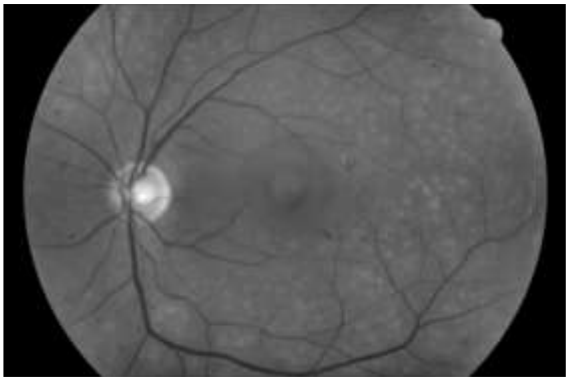

Figure 3: Lesion extraction – input green color band after resizing

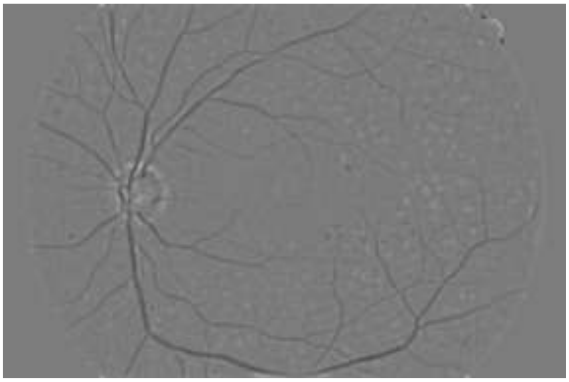

Figure 4: Lesion extraction – Difference Image

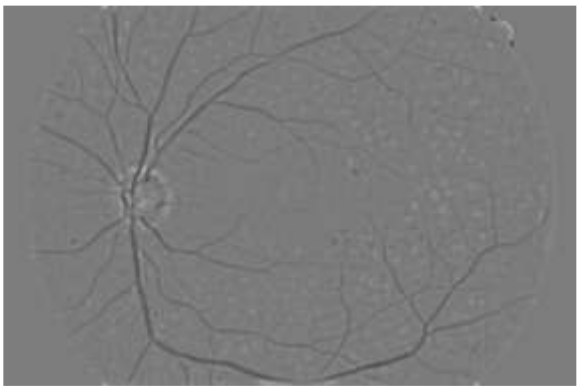

Figure 5: Lesion extraction – Normalized Image

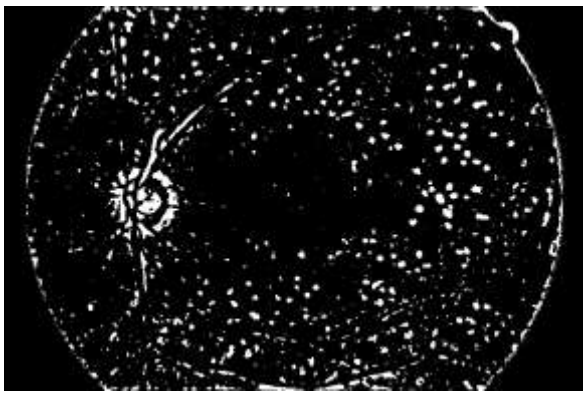

Figure 6: Lesion extraction – Lesion Candidates

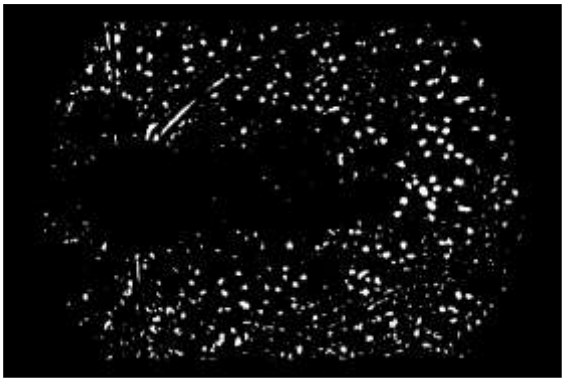

Figure 7: Removing False Lesion Candidates – After Applying Mask

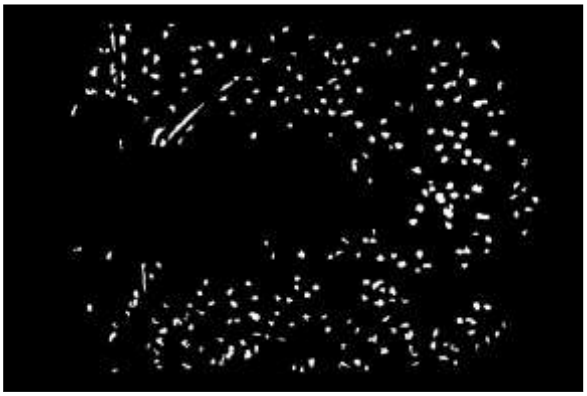

Figure 8: Removing False Lesion Candidates – Removing Noise

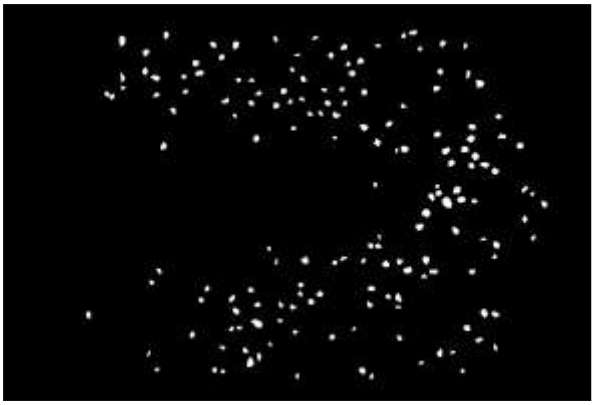

Figure 9: Removing False Lesion Candidates – Final Mask

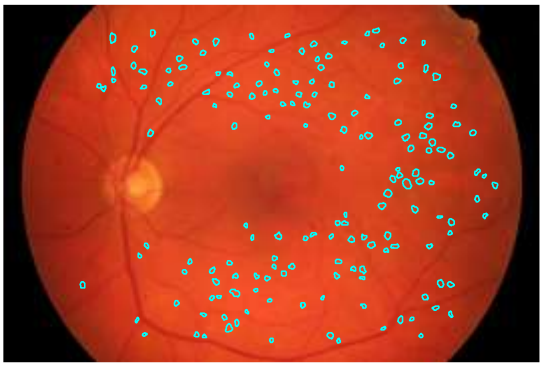

Figure 10: Removing False Lesion Candidates – Detected Lesion

Table 1: Performance evaluation of proposed approach using various feature extraction techniques with DRIVE image dataset

Parameters	HOG	LBP	Hybrid Features
Accuracy	93.45%	94.02%	96.83%
Error Rate	6.55%	5.98%	3.17%
Sensitivity	93.45%	94.02%	96.83%
Specificity	96.50%	97.10%	99.06%
Precision	93.40%	94.32%	96.70%
False Positive Rate	3.50%	2.90%	0.94%
F1-Score	93.42%	94.17%	96.76%
MCC	90.54%	92.18%	96.00%
Kappa Statistics	86.26%	87.61%	91.98%

Table 1 shows the performance of HOG, LBP, and Hybrid Features on the DRIVE dataset. Hybrid Features achieved the highest accuracy at 96.83%, followed by LBP at 94.02% and HOG at 93.45%. Hybrid Features also had the lowest error rate (3.17%), the highest specificity (99.06%), and the best F1-Score (96.76%). Precision, MCC, and Kappa Statistics were similarly highest for Hybrid Features, confirming its superior performance across all metrics.

Table 2: Performance Evaluation of Proposed Approach Using Various Feature Extraction Techniques with Fundus Image Registration Dataset

Parameters	HOG	LBP	Hybrid Features
Accuracy	89.45%	90.02%	93.45%
Error Rate	10.55%	9.98%	6.55%
Sensitivity	89.45%	90.02%	93.45%
Specificity	92.50%	93.10%	96.50%
Precision	89.40%	90.32%	93.40%
False Positive Rate	7.50%	6.90%	3.50%
F1-Score	89.42%	90.17%	93.42%
MCC	86.20%	88.39%	92.10%
Kappa Statistics	81.00%	82.61%	87.26%

Table 2 presents the results for the Fundus Image Registration dataset. Again, Hybrid Features outperformed HOG and LBP, with 93.45% accuracy and a 6.55% error rate. It also led in sensitivity, specificity, precision, and F1-Score, further emphasizing its robustness. MCC and Kappa Statistics were highest for Hybrid Features, demonstrating its effectiveness in classifying retinal images for diabetic retinopathy.

Table 3: Comparative analysis of NN and SCA-NN approach

Parameters	Neural Network Classifier	SCA-Optimized Neural Network Classifier
Accuracy	93.88%	96.83%
Error Rate	6.12%	3.17%
Sensitivity	93.88%	96.83%
Specificity	96.96%	99.06%

Precision	93.92%	96.70%
False Positive Rate	3.04%	0.94%
F1-Score	93.90%	96.76%
MCC	91.76%	96.00%
Kappa Statistics	87.08%	91.98%

Table 3 compares a Neural Network Classifier with an SCA-Optimized Neural Network (SCA-NN). The SCA-NN significantly outperformed the standard Neural Network, with an accuracy of 96.83% versus 93.88%, a lower error rate (3.17%), and higher scores across sensitivity, specificity, and precision, F1-Score, MCC, and Kappa Statistics.

Table 4: Comparison of the proposed approach with previous research works

Parameters	KNN [16]	RF [17]	SCA-Optimized Neural Network Classifier
Accuracy	94.44%	96.67%	96.83%
Error Rate	5.56%	3.33%	3.17%
Sensitivity	94.44%	96.67%	96.83%
Specificity	98.15%	98.89%	99.06%
Precision	95.45%	96.82%	96.70%
False Positive Rate	1.85%	1.11%	0.94%
F1-Score	94.56%	96.69%	96.76%
MCC	93.05%	95.62%	96.00%
Kappa Statistics	85.19%	91.11%	91.98%

Table 4 contrasts the SCA-Optimized Neural Network with KNN and Random Forest (RF). The SCA-NN achieved the highest accuracy (96.83%), sensitivity, specificity, and precision, with a lower error rate (3.17%) than KNN and RF. Its MCC and Kappa Statistics were also the best, underscoring its superior performance in diabetic retinopathy detection.

5. CONCLUSION

This study proposes a robust method for diabetic retinopathy (DR) detection and classification by combining advanced image processing and an optimized machine-learning model. The approach includes contrast enhancement, Gabor filtering for vessel extraction, and dual feature extraction using HOG and LBP to capture detailed retinal image information. A key innovation is optimizing the neural network classifier with the Sine Cosine Algorithm (SCA), which improves accuracy, precision, and sensitivity. Evaluations on the DRIVE and Fundus Image Registration datasets show significant improvements, with classification accuracies of 93.2% for the Feedforward Neural Network and 96.83% for the SCA-Optimized Neural Network. This approach sets a new benchmark for automated DR diagnosis, offering a scalable framework for future research in medical image analysis.

Acknowledgments

The authors would like to express their gratitude to SAGE University, Indore, Madhya Pradesh for all of their assistance and encouragement in carrying out this research and publishing this paper.

REFERENCES

[1] Abdel Maksoud, E., Barakat, S., & Elmogy, M. (2022). A comprehensive diagnosis system for early signs and different diabetic retinopathy grades using fundus retinal images based on pathological changes detection. Computers in Biology and Medicine, 126, 104039.

[2] Frazao, L. B., Theera-Umpon, N., & Auephanwiriyakul, S. (2024). Diagnosis of diabetic retinopathy based on holistic texture and local retinal features. Information Sciences, 475, 44–66.

[3] Wu, Z., Shi, G., Chen, Y., Shi, F., Chen, X., Coatrieux, G., Yang, J., Luo, L., & Li, S. (2022). Coarse- to-fine classification for diabetic retinopathy grading using convolutional neural network. Artificial Intelligence in Medicine, 108(January), 101936.

[4] Momeni Pour, A., Seyedarabi, H., Abbasi Jahromi, S. H., & Javadzadeh, A. (2022). Automatic Detection and Monitoring of Diabetic Retinopathy Using Efficient Convolutional Neural Networks and Contrast Limited Adaptive Histogram Equalization. IEEE Access, 8, 136668– 136673.

[5] Saxena, G., Verma, D. K., Paraye, A., Rajan, A., & Rawat, A. (2022). Improved and robust deep learning agent

for preliminary detection of diabetic retinopathy using public datasets. Intelligence-Based Medicine, 3–4(June), 100022.

[6] Katada, Y., Ozawa, N., Masayoshi, K., Ofuji, Y., Tsubota, K., & Kurihara, T. (2022). Automatic screening for diabetic retinopathy in interracial fundus images using artificial intelligence. Intelligence-Based Medicine, 3–4(July), 100024.

[7] Nguyen, Q. H., Muthuraman, R., Singh, L., Sen, G., Tran, A. C., Nguyen, B. P., & Chua, M. (2022). Diabetic Retinopathy Detection using Deep Learning. Proceedings of the 4th International Conference on Machine Learning and Soft Computing, 16(3), 103–107.

[8] Dutta, S., Manideep, B. C. S., Basha, S. M., Caytiles, R. D., & Iyengar, N. C. S. N. (2023). Classification of Diabetic Retinopathy Images by Using Deep Learning Models. International Journal of Grid and Distributed Computing, 11(1), 99–106.

[9] R C, K., Ankalaki, S., & Majumdar, J. (2022). A Study of Performance Evaluation of Convolution Neural Network for Diabetic Retinopathy. International Journal of Advanced Trends in Computer Science and Engineering, 9(4), 5009–5014.

[10] Zhou, L., Zhao, Y., Yang, J., Yu, Q., & Xu, X. (2023). Deep multiple instance learning for automatic detection of diabetic retinopathy in retinal images. IET Image Processing, 12(4), 563–571.

[11] Sangeethaa, S. N., & Uma Maheswari, P. (2023). An Intelligent Model for Blood Vessel Segmentation in Diagnosing DR Using CNN. Journal of Medical Systems, 42(10), 175.

[12] Li, F., Liu, Z., Chen, H., Jiang, M., Zhang, X., & Wu, Z. (2024). Automatic Detection of Diabetic Retinopathy in Retinal Fundus Photographs Based on Deep Learning Algorithm. Translational Vision Science & Technology, 8(6), 4.

[13] Mobeen-ur-Rehman, Khan, S. H., Abbas, Z., & Rizvi, S. D. (2024). Classification of Diabetic Retinopathy Images Based on Customised CNN Architecture. 2024 Amity International Conference on Artificial Intelligence (AICAI), 244–248.

[14] Butt, M. M., Latif, G., Iskandar, D. N. F. A., Alghazo, J., & Khan, A. H. (2024). Multi-channel Convolutions Neural Network Based Diabetic Retinopathy Detection from Fundus Images. Procedia Computer Science, 163, 283–291.

[15] Afrin, R., & Shill, P. C. (2024). Automatic Lesions Detection and Classification of Diabetic Retinopathy Using Fuzzy Logic. 2024 International Conference on Robotics, Electrical and Signal Processing Techniques (ICREST), 527–532.

[16] Rehman, A., Harouni, M., Karimi, M., Saba, T., Bahaj, S.A. and Awan, M.J., 2022. Microscopic retinal blood vessels detection and segmentation using support vector machine and K-nearest neighbors. Microscopy research and technique, 85(5), pp.1899-1914.

[17] Chowdhury, A.R., Chatterjee, T. and Banerjee, S., 2024. A random forest classifier-based approach in the detection of abnormalities in the retina. Medical & biological engineering & computing, 57, pp.193-203.